Kinetics and Mechanism of the Carbonate Ion Inhibited Aqueous Ozone Decomposition

Attila Nemes,[†,‡] István Fábián,[*,†] and Rudi van Eldik[‡]

Department of Inorganic and Analytical Chemistry, University of Debrecen, POB 21, H-4010, Debrecen, Hungary, and Institute for Inorganic Chemistry, University of Erlangen-Nürnberg, Egerlandstr. 1, 91058 Erlangen, Germany

Received: March 14, 2000; In Final Form: June 15, 2000

The carbonate ion inhibited aqueous decomposition of ozone was studied by the stopped-flow method at 25.0 ± 0.1 °C in 0.5 M $NaClO_4$. It was shown that the rate of decomposition sharply decreases and reaches a limiting value by increasing the carbonate ion concentration. A detailed kinetic model was developed for the interpretation of the results. The corresponding set of rate constants was calculated by simultaneously fitting kinetic traces obtained at the absorption maxima of O_3 (260 nm), O_3^- (430 nm), and CO_3^- (600 nm). It was confirmed that the inhibition is mainly due to the removal of two dominant chain carrier radicals, OH and O_3^-, via the following reaction steps: $CO_3^{2-} + OH \rightarrow CO_3^- + OH^-$, $k = (1.0 \pm 0.1) \times 10^8$ M^{-1} s^{-1}, and $CO_3^- + O_3^- \rightarrow CO_3^{2-} + O_3$, $k = (5.5 \pm 0.5) \times 10^7$ M^{-1} s^{-1}. The kinetically less significant reactions of other transient species are also discussed in detail. The mechanism gives proper description of ozone decay, the formation and subsequent disappearance of ozonide ion and carbonate ion radicals, as well as the concentration change of other intermediates over the pH range 10.7−12.8. The model predicts that ozone decomposition occurs in a simple first-order process at high CO_3^{2-} concentration, in agreement with the experimental data.

Introduction

The extreme oxidizing power of ozone is frequently utilized in practical applications, such as water and wastewater treatment, disinfection, bleaching, and advanced oxidation technologies.[1,2] Ozone can directly or indirectly react with the substrates in these processes. In the direct oxidation, typically first ozonides are formed which undergo decomposition into various radicals in subsequent reaction steps. Indirect oxidation reactions are associated with the decomposition of ozone, which can be approximated by the following simple stoichiometry:

$$2O_3 = 3O_2 \qquad (1)$$

Nevertheless, the decomposition is a complex, radical chain reaction, and the actual oxidizing agents are the radicals formed in this process.[3−15] Quite often the alternative paths of the oxidation occur simultaneously, and their relative significance can be controlled to some degree by selecting appropriate experimental parameters. It is essential to clarify how reactive intermediates are generated in these reactions and how their concentrations can be optimized under specific conditions. Promoters, including irradiation with UV light and/or inhibitors, provide a convenient way to adjust the concentrations of the reactive species in the reaction mixtures.[6,8,13−17]

Carbonate ion is one of the most efficient inhibitors of ozone decomposition and it is used to stabilize ozone solutions in industrial applications.[16] Because of the relatively high CO_3^{2-} content of natural waters, the effect of carbonate ion on ozone lifetime is also a subject of interest in water treatment technologies. Despite extensive studies in this field, only formal descriptions of the carbonate inhibition have been reported before. Several attempts were made to identify the most important inhibition steps,[8,13] but a mechanism accounting for all the details has not been developed so far.

In earlier studies, the carbonate inhibition was attributed to scavenging the hydroxyl radical:[8,13,17]

$$CO_3^{2-} + OH = CO_3^- + OH^- \qquad (2)$$

Because OH is one of the most significant chain carriers in aqueous ozone decomposition, its removal certainly affects the kinetics of ozone decay. However, model calculations indicated that reaction 2 alone is not sufficient for the interpretation of the carbonate ion effect.[9] Additional reaction steps had to be considered in the model to account for the fate of the reactive CO_3^- radical. It was concluded that the main reaction of this species occurs with the O_3^- radical,[9]

$$CO_3^- + O_3^- = CO_3^{2-} + O_3 \qquad (3)$$

The rate constants for reactions 2 and 3 were reported in previous literature.[18,19] The inclusion of these reactions as well as several minor reaction steps into the model led to a proper description of the general features of carbonate ion inhibition.[9,10] Nevertheless, the conclusions of the model calculations required further confirmation on the basis of systematically designed kinetic experiments.

The results presented here are based on a series of new stopped-flow (SF) experiments over an extended pH and $[CO_3^{2-}]_{tot}$ range. The main objectives of this work were to test experimentally the validity of the previously proposed kinetic model for carbonate inhibition,[9] to identify the most significant reaction steps, and to provide a suitable set of rate constants for simulating the kinetic traces. Recently we have reported a

* Corresponding author: Tel: (+36 52) 512 900, ext 2378. Fax: (+36 52) 489 667. E-mail: ifabian@delfin.klte.hu.
† University of Debrecen.
‡ University of Erlangen-Nürnberg.

10.1021/jp000972t CCC: $19.00
Published on Web 08/05/2000

detailed mechanism (NFG model) for the noninhibited ozone decomposition.[12] It was consistent with the experimental observations and gave excellent estimates for the measured lifetimes of ozone over the pH range 10.4−13.2. Thus, the NFG model was used as a basis for further model development in the present study.

Experimental Section

Reagents. Ozone solutions were prepared and handled as described before.[11,12] The decomposition of ozone was triggered by mixing slightly acidic ozone stock solutions with NaOH solution containing Na_2CO_3 (Fluka, analytical grade) at appropriate concentration levels. The total carbonate ion concentration of the reaction mixtures, $[CO_3^{2-}]_{tot}$, was varied between 1.0×10^{-5} and 4.0×10^{-3} M. The ionic strength was set to 0.5 M with $NaClO_4$ (Fluka), which was recrystallized from water. The ozone concentration was around 10^{-4} M. The pH, defined as $-\log[H^+]$ throughout this paper, was calculated from the acid, base, and sodium carbonate concentrations of the reactants. The literature values for the equilibrium constants were corrected to an ionic strength of 0.5 M. The decomposition was studied in the pH range 10.7−12.8.

For the preparation of all stock and sample solutions, water was doubly deionized and ultrafiltered in a MILLI-Q RG (Millipore) purification system ($R_{H_2O} \geq 18$ MΩ cm) and finally freshly distilled in an all-glass still.

All experiments were made at an oxygen concentration of $\sim 7.5 \times 10^{-4}$ M, which was measured with a Biolytik oxygen-detection system.

Methods. Kinetic measurements were performed on an Applied Photophysics DX-17 MV sequential stopped-flow spectrometer with 10 mm optical path. For rapid-scan measurements an Applied Photophysics photodiode array detector was connected to the same SF apparatus. The dead time of the instrument was determined to be 1.1 ± 0.1 ms by using the DCIP−L-ascorbic acid method.[20] The background absorbance was set to 0.000 ± 0.001 using a 2.0×10^{-4} M $HClO_4$ (I = 0.5 M $NaClO_4$) solution as a reference. The entrance and exit slit widths of the monochromator were set such that photochemical decomposition of ozone had negligible contribution to the observed kinetic process.[12] The reactants were mixed in a 1:1 ratio.

The decomposition was monitored at 260, 430, and 600 nm, and 25.0 ± 0.1 °C. At these wavelengths ozone, the ozonide ion,[4,12,13,21,22] and carbonate ion[23] radicals have maximum absorbance, respectively. Nine subsequent measurements (three at each wavelength) formed one series. The three traces obtained at a particular wavelength were averaged. The corresponding traces were reproducible within ±0.005 AU. Each series of the measurements was made within 5 min after preparing the ozone stock solution and without refilling the SF syringes. This protocol was used to minimize ozone loss from the samples and to ensure that the kinetic traces at the three wavelengths corresponded to the same initial ozone concentration. Ozone decomposition in the drive syringes of the SF instrument was negligible and the ozone concentration was constant within ±1.5% in a series.

Data Fitting. The time scales of the kinetic curves were corrected with the dead time of the SF apparatus, and the number of the experimental data points (typically 400 points per trace) was reduced to one-fourth by smoothing each trace with a spline algorithm. Calculations were made with the modified data sets by simultaneously fitting 32 traces, altogether using approximately 3500 data points. The traces included 22 curves at 260 nm from the 10.4−12.8 pH range, five curves at 430 nm at pH 12.5 and 12.8, and five curves at 600 nm at pH 11.5 and 12.2.

TABLE 1: Molar Absorption Coefficients (in M^{-1} cm^{-1}) Used in the Calculations

species	at 260 nm	at 430 nm	at 600 nm	ref
O_3	3135	0	0	11
O_2^-	2000	0	0	4
O_3^-	0	2000	0	4
HO_2^-	164	0	0	11
H_2O_2	13.9	0	0	11
OH^-	0.027	0	0	11
OH	405	0	0	4
HO_2	500	0	0	4
CO_3^-	0	0	1860	23

In the fitting procedure, the kinetic model was represented by an ordinary differential equation system (ODE). It was assumed that each reaction step is elementary. The ODE was integrated with the program package ZITA[24] by using the GEAR algorithm,[25] and the concentration−time profiles were calculated for each species. Molar absorbances taken from the literature or determined in our earlier studies were used to calculate the absorbance in each point (see Table 1). The rate constants were estimated by minimizing the difference between the measured and calculated absorbances.[24] Further details on the data fitting are given in the Discussion.

Results

The shape of the experimental kinetic traces and the decomposition rate of ozone strongly depend on the pH and carbonate ion concentration. Typical kinetic curves are shown in Figure 1.

In the absence of carbonate ion and at high pH the SF traces at 260 nm show composite kinetic features (Figure 1a, inset). After a sharp initial decrease, the absorbance slightly increases and remains constant for several minutes. Under such conditions the superoxide ion radical, O_2^-, is formed in relatively high concentration ($\sim 10^{-5}$ M).[12,13] Thus, the superposition of the spectral effects due to ozone decomposition and the formation of O_2^- produces the characteristic minimum in the kinetic traces. The decrease in pH and the increase in $[CO_3^{2-}]_{tot}$ have practically the same effect on the kinetic curves. As the pH is decreased and/or $[CO_3^{2-}]_{tot}$ is increased, the sharp minimum disappears and the final absorbance approaches zero. This trend clearly indicates that the O_2^- production becomes less significant at low pH and high carbonate ion concentration. For example, at pH <12.0 or at pH 12.8 and $[CO_3^{2-}]_{tot} > 1.5$ mM the final absorbance is zero. At the same time, the half-life of ozone increases by lowering the pH and, in agreement with previous reports,[13] reaches a limit as a function of $[CO_3^{2-}]_{tot}$. The smaller the pH, the smaller carbonate ion concentration is required to reach the limiting value (Figure 2).

To a certain extent very similar trends are observed for the formation and subsequent decay of the O_3^- radical. The yield of this species decreases by decreasing the pH and increasing $[CO_3^{2-}]_{tot}$ (Figure 1b).

The formation and decomposition of a third intermediate, the CO_3^- radical, could be monitored at 600 nm over the whole pH range studied.[8,13] Its maximum concentration corresponds to only a slightly higher absorbance change (0.006 AU) than the experimental error of the absorbance measurements. Nevertheless, the kinetic traces are fairly reproducible and clearly show the formation of this species (Figure 1c). The concentration of CO_3^- varies with the initial ozone concentration, pH, and

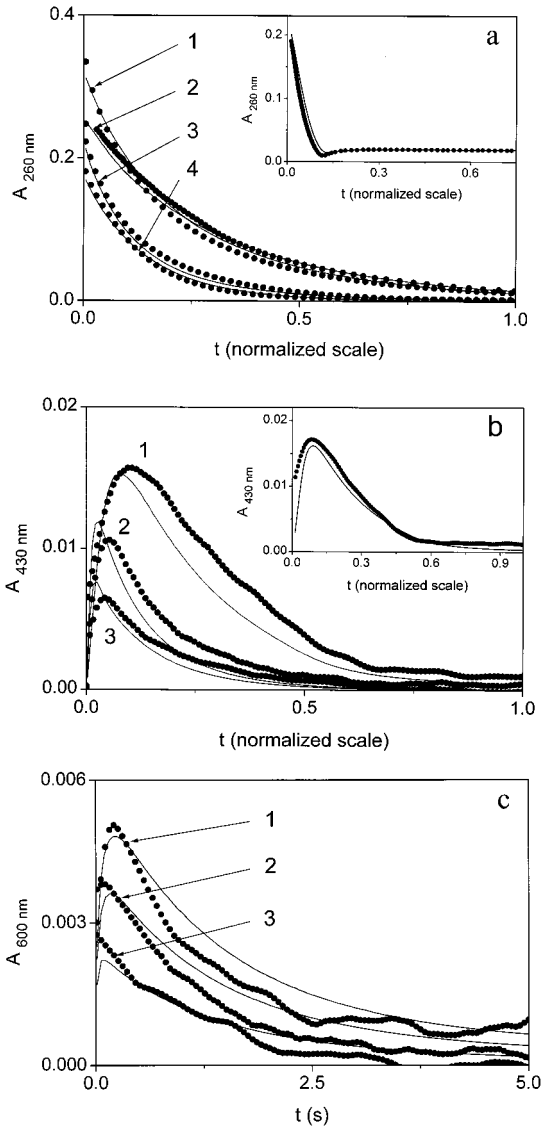

Figure 1. Experimental (●) and calculated (−) traces for carbonate ion inhibited ozone decomposition (t = 25 °C, I = 0.5 M $NaClO_4$, $[O_3]_0 = (5.8 \times 10^{-5}) - (1.1 \times 10^{-4}$ M). (a) Ozone decay recorded at 260 nm: (1) pH 10.7, $[CO_3^{2-}]_{tot} = 5.0 \times 10^{-5}$ M (unit time, 10 s); (2) pH 12.8, $[CO_3^{2-}]_{tot} = 3.0 \times 10^{-3}$ M (0.1 s); (3) pH 11.5, $[CO_3^{2-}]_{tot} = 5.0 \times 10^{-5}$ M (2.5 s); (4) pH = 11.8, $[CO_3^{2-}]_{tot} = 4.0 \times 10^{-3}$ M (2.5 s). Inset: Kinetic trace in the absence of added carbonate ion, pH 13.2 (0.2 s). (b) The formation and disappearance of O_3^- at 430 nm, pH 12.5: (1) $[CO_3^{2-}]_{tot} = 1.0 \times 10^{-5}$ M (unit time, 0.2 s); (2) $[CO_3^{2-}]_{tot} = 5.0 \times 10^{-4}$ M (0.5 s); (3) $[CO_3^{2-}]_{tot} = 1.0 \times 10^{-3}$ M (5.0 s). Inset: Kinetic trace in the absence of added carbonate ion, pH 12.5 (0.2 s) (c) The formation and disappearance of CO_3^- at 600 nm, pH 11.5: (1) $[CO_3^{2-}]_{tot} = 4.0 \times 10^{-3}$ M; (2) $[CO_3^{2-}]_{tot} = 1.5 \times 10^{-3}$ M; (3) $[CO_3^{2-}]_{tot} = 5.0 \times 10^{-4}$ M.

CO_3^{2-} concentration in a complex way. Higher $[CO_3^{2-}]_{tot}$ or higher initial ozone concentration yields a higher CO_3^- concentration. The rate of CO_3^- decay is accelerated by increasing the pH.

In earlier studies, noninhibited ozone decomposition at pH >12 was interpreted in terms of a simple rate law which was first-order with respect to both O_3 and OH^-.[13,26,27] In less alkaline solution the rate expression was extended with a second-order term with respect to O_3.[8] It was shown recently that these expressions are of limited use and a simple rate law could not be derived for the interpretation of the kinetic traces in the pH range 10.4−13.2.[12] The complex kinetic feature of the reaction vanishes when the carbonate ion concentration is increased. At

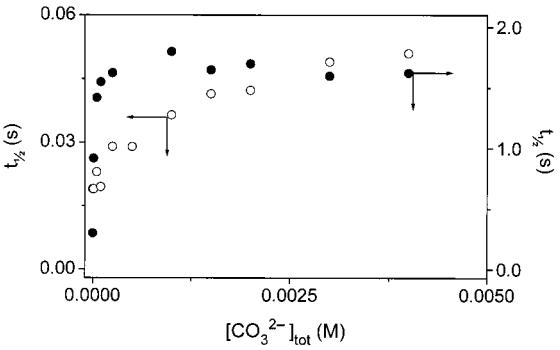

Figure 2. Half-life of ozone vs $[CO_3^{2-}]_{tot}$ at pH 12.5 (○) and 10.7 (●). $[O_3]_0 = (5.2 \times 10^{-5}) - (1.3 \times 10^{-4})$ M, t = 25 °C, I = 0.5 M $NaClO_4$.

TABLE 2: The NFG Model for Aqueous Ozone Decomposition[12]

reaction		rate constant	ref
$O_3 + OH^- = HO_2^- + O_2$	k_{A1}	140 M^{-1} s^{-1}	12
$HO_2^- + O_3 = O_3^- + HO_2$	k_{A2}	5.5×10^6 M^{-1} s^{-1}	6
$O_2^- + O_3 = O_3^- + O_2$	k_{A3}	$> 3.0 \times 10^8$ M^{-1} s^{-1}	12
$O_3^- + OH = O_2^- + HO_2$	k_{A4}	2.0×10^{10} M^{-1} s^{-1}	12
$O_3^- + OH = O_3 + OH^-$	k_{A5}	8.3×10^9 M^{-1} s^{-1}	12
$OH + O_3 = HO_2 + O_2$	k_{A6}	2.5×10^7 M^{-1} s^{-1}	12
$O^- + HO_2^- = O_2^- + OH^-$	k_{A7}	3.2×10^9 M^{-1} s^{-1}	12
$O^- + O_2^- (+ H_2O) = O_2 + 2OH^-$	k_{A8}	1.8×10^8 M^{-1} s^{-1}	12
$O_3^- = O_2 + O^-$	k_{A9}	5.0×10^3 s^{-1}	12
($\log K = -5.7$)	k_{-A9}	2.6×10^9 M^{-1} s^{-1}	12
$HO_2 + OH^- = O_2^- (+ H_2O)$	k_{A10}	1.0×10^{10} M^{-1} s^{-1}	*a*
($\log K = 9.0$)	k_{-A10}	10 s^{-1}	*b*
$H_2O_2 + OH^- = HO_2^- (+ H_2O)$	k_{A11}	1.0×0^{10} M^{-1} s^{-1}	*a*
($\log K = 2.1$)	k_{-A11}	7.6×0^7 s^{-1}	*b*
$OH + OH^- = O^- (+ H_2O)$	k_{A12}	4.0×10^{10} M^{-1} s^{-1}	28
($\log K = 1.9$)	k_{-A12}	5.4×10^8 s^{-1}	*b*
$H^+ + OH^- = (H_2O)$	k_{A13}	1.0×10^{11} M^{-1} s^{-1}	29
($\log K = 13.77$)	k_{-A13}	1.7×10^{-3} Ms^{-1}	*b*

[a] Assuming diffusion control. [b] Calculated from the forward rate constant and the equilibrium constant.

260 nm, simple first-order kinetic traces were observed when the limiting value of the ozone lifetime was reached.

Discussion

The Kinetic Model. In alkaline solution, ozone decomposition is triggered by a direct reaction between O_3 and OH^-, and the overall process proceeds via a series of propagation steps. Recently we have identified the most important chain carrier radicals and proposed a minimum set of reactions for the interpretation of the kinetic results in the absence of catalysts and inhibitors.[11,12] Although some of these steps may prove to be negligible in the presence of carbonate ion, the NFG model was accepted without modifications in the present study. The corresponding rate constants were included in the calculations with fixed values as given in Table 2.

The kinetic model for carbonate inhibition was constructed by following the protocol described in our previous reports.[11,12] First, the NFG model was extended with appropriate reaction steps taken from the literature (Table 3).[6,18,19,30−34] Earlier reported rate constants for some of these reactions differ by more than an order of magnitude. In part, this may reflect that their values were determined under significantly different experimental conditions. A further source of the noted discrepancies could be the use of simplified kinetic models for the evaluation of the experimental data. Because of strong kinetic coupling among various reaction steps, the simplifications could

TABLE 3: Extension of the NFG Model for Carbonate Ion Inhibited Ozone Decomposition

reaction[a]		rate constant (in M^{-1} s^{-1})		ref[b]
		calculated	literature	
$HCO_3^- + OH^- = CO_3^{2-} (+ H_2O)$	k_{B1}	5.0×10^9 [c]	5.0×10^9	10
$(\log K = 3.47)$[d]	k_{-B1}	1.7×10^6 [e]	1.0×10^6	*f*
$CO_3^{2-} + OH = CO_3^- + OH^-$	k_{B2}	$(1.0 \pm 0.1) \times 10^8$	$(2.0-4.2) \times 10^8$	17, 23
$CO_3^- + O_3^- = CO_3^{2-} + O_3$	k_{B3}	$(5.5 \pm 0.5) \times 10^7$	6.0×10^7	18
$CO_3^{2-} + O^- (+ H_2O) = CO_3^- + 2OH^-$	k_{B4}	$<1.0 \times 10^7$ [g]	1.0×10^7	31
$HCO_3^- + OH = CO_3^- (+ H_2O)$	k_{B5}	$<2 \times 10^7$ [g]	$(8.5 \times 10^6) - 4.9 \times 10^7$	30, 33
$HCO_3^- + O_2^- = CO_3^- + HO_2^-$	k_{B6}	$(4.0 \pm 1.5) \times 10^6$ [g]	$(1.0 - 2.0) \times 10^6$	34, 31
$CO_3^- + O_2^- = CO_3^{2-} + O_2$	k_{B7}	$(8.7 \pm 0.4) \times 10^7$	$(4.0 \times 10^8) - (1.5 \times 10^9)$	32, 31
$CO_3^- + H_2O_2 = HCO_3^- + HO_2$	k_{B8}	$(7.6 \pm 0.7) \times 10^8$	8.0×10^5	32
$CO_3^- + HO_2^- = CO_3^{2-} + HO_2$	k_{B9}	$<1.0 \times 10^8$ [g]	6.0×10^7	32
$2CO_3^- + 2OH^- = 2CO_3^{2-} + H_2O_2$	k_{B10}		7.0×10^7 [h]	31
$CO_3^- + O^- (+ H_2O) = CO_3^{2-} + H_2O_2$	k_{B11}		1.0×10^7	31

[a] Reactions under the dashed line were rejected from the model. [b] References are given for the lower and upper literature value. [c] Assuming diffusion control. [d] Original value is corrected for $I = 0.5$ M $NaClO_4$. [e] Rate constant is given in s^{-1}. [f] $k_{-B1} = k_{B1}/K_{B1}$. [g] The rate constant is estimated on the basis of simulations. [h] Rate constant is given in M^{-2} s^{-1}.

easily yield improper rate expressions and biased estimates for the kinetic parameters. To avoid this problem, a comprehensive data treatment was used in the present study, and all relevant rate constants with respect to carbonate inhibition were evaluated simultaneously.

With the exception of step B1, the kinetic role of each step in Table 3 was analyzed by sensitivity analysis. The rate constant of the tested reaction was systematically varied up to the diffusion controlled limit (10^{10} M^{-1} s^{-1}) and the kinetic traces were simulated in every case. When the shapes of the kinetic curves were not affected even at the highest value of the rate constant, the given step was considered to be kinetically unimportant and was rejected from the model. Such reactions are B10 and B11. Step B1 is a simple proton-transfer reaction which accounts for the speciation of carbonate ion as a function of pH. In the case of simple acids and bases, these reactions are diffusion controlled and, in agreement with previous considerations,[10] $k_{B1} = 5.0 \times 10^9$ M^{-1} s^{-1} was used for the forward reaction. The reverse rate constant was replaced with k_{B1}/K_{B1} in the calculations.

After determining the basic set of reactions, the kinetic traces were simulated by using the literature rate constants for each step as listed in Table 3. Because the agreement between measured and calculated traces was not satisfactory, the rate constants were systematically varied until a better fit was obtained. In this way a relatively good initial set of parameters was obtained for the curve fitting. An attempt was made to estimate $k_{B2} - k_{B9}$ by using a combination of numeric integration and least-squares fitting method. The rate constants for the kinetically dominant reaction steps could be fitted with a relatively small error (<10%). The uncertainty of other rate constants was much larger, and their values could be changed within a relatively wide range without significantly affecting the goodness of the fit. The most likely values for these parameters were determined by simulations.

The noted ambiguity of several rate constants is due to experimental limitations which did not allow us to select appropriate conditions for the determination of each parameter. In thermally induced ozone decomposition, the initial concentration of the reactive intermediates cannot be varied and the concentration dependencies of the reaction rate can be studied only for a few components. As a consequence, the kinetic traces do not carry enough information for the rate constants of those reaction steps which play a minor role in the overall reaction. It should be added that these steps may become dominant under specific conditions where the chain carrier radicals are generated at relatively high concentration levels.

In most cases, the rate constants reported here agree with the literature data within an order of magnitude. In general, the agreement with earlier results seems to be acceptable, in particular if we consider that many of the rate constants reported earlier were determined in pulse radiolysis experiments.[19,30,32] In those kinetic studies the reactive intermediates were produced at several orders of magnitude higher concentration levels than in thermal decomposition of ozone, and the actual composition of the reaction mixtures was also different from the ones used here. These factors may account for even more significant deviations between the literature data and our results. The only exception is reaction B8, for which a $\sim 10^3$ times higher value was found than before.[32] The source of this discrepancy is not apparent. Clearly, the differences in the experimental conditions cannot account for such a large deviation in the rate constants. As will be discussed in detail, according to our calculations k_{B8} needs to be on the order of 10^8 M^{-1} s^{-1} to obtain a reasonable fit of the experimental data. The model predicts the trends of the experimental kinetic traces reasonably well with the rate constants given in Table 3. The agreement between measured and calculated kinetic traces is illustrated in Figure 1.

The model proposed here confirms previous conclusions and leads to a better understanding of the carbonate ion inhibited ozone decomposition. As suggested before,[8,13] reaction B2 is one of the most important steps in the mechanism. However, the removal of the OH radical alone is not enough to retard the decomposition when the pH is increased. According to our recent results, a mechanistic changeover occurs in the decomposition from pH 10.4 to 13.2. In very alkaline solution, pH >12.5, about 70% of ozone is consumed in reactions A1 and A2, and O_3^- becomes the main chain carrier species instead of OH. According to the NFG model, O_3^- is generated in reaction sequence A1−A3, and the reactions of the hydroxyl radical do not contribute directly to the formation of this species, rather it slightly decreases $[O_3^-]$ via steps A4 and A5 (Table 2). Thus, scavenging only the OH radical by carbonate ion should not affect, or even increase, the concentration of O_3^-. The kinetic traces at 430 nm show quite an opposite trend as a function of $[CO_3^{2-}]_{tot}$ (Figure 1b). To account for carbonate inhibition at high pH and for the removal of O_3^-, the inclusion of step B3 into the model seems to be essential though this reaction has a smaller effect than B2. Step B3 affects the overall reaction in a complex way. It removes a reactive intermediate, at least in part accounts for the decay of the carbonate ion radical, and regenerates ozone.

With steps B2 and B3, the model gave satisfactory interpretation of the main trends observed experimentally in the kinetic

traces and lifetimes of ozone. However, the calculated concentration profiles for CO_3^- were not fully consistent with the experimental data. At the characteristic spectral band of CO_3^-, $\lambda_{max} = 600$ nm, the model predicted an about 4 times larger than measured absorbance which never dropped to zero at the end of the reaction. Very similar problems were observed with the kinetic profiles for O_2^-. The disappearance of the sharp minimum in the kinetic traces at 260 nm indicates that O_2^- is formed below the detection limit at high carbonate ion concentrations. In contrast, calculated final concentrations of the superoxide radical were on the order of $10^{-6}-10^{-5}$ M, which would correspond to absorbances up to 0.01 AU.

The discrepancies could be eliminated by including reactions B4−B9 in the model. Superoxide radical is produced in the reactions of OH, O_3^-, O^- (steps A2, A4, A6), and quenching any of these species would reduce the O_2^- concentration. B2−B7 are such reactions. Although B4, B5, and B6 also produce CO_3^-, these steps need to be considered to calculate the proper concentration profiles for O_2^-. Steps B8 and B9 are essential to remove the carbonate ion radical, but they also produce HO_2, which immediately deprotonates to O_2^- in the entire pH range studied.

Because of the large deviation of k_{B8} from the literature value,[32] the validity of the rate constant obtained by the least-squares fitting method was tested by sensitivity analysis. When the literature value was used for k_{B8}, 8.0×10^5 M^{-1} s^{-1}, a nonzero final absorbance was calculated at 600 nm, i.e., the model predicted that the carbonate ion radical exists at observable concentration levels for an extended period of time. This result contradicts the experimental observations. Because step B8 becomes the main reaction channel for quenching the carbonate ion radical in the final stage of the decomposition, the calculated kinetic profiles for CO_3^- are sensitive to k_{B8}. Model calculations confirmed that complete removal of CO_3^- within the time scale observed experimentally requires k_{B8} to be around 8×10^8 M^{-1} s^{-1}. This conclusion is in line with the results obtained by the fitting procedure. With the rate constants listed in Tables 2 and 3, an appropriate balance could be set between the competing and kinetically strongly coupled reaction paths and the experimental kinetic traces could be reproduced reasonably well.

A Simplified Model. As it was discussed before, ozone lifetime reached a limiting value at high carbonate ion concentration and simple first order-kinetic traces were observed at 260 nm. This feature of the system can be interpreted by assuming that the main chain carrier species are completely quenched by carbonate ion in the limiting region. As a consequence, the chain length of the decomposition is reduced to the shortest possible reaction sequence, and kinetic coupling between the remaining propagation steps is completely eliminated. Under such conditions, a simplified model is suitable for the interpretation of the data in which the rate-determining step is reaction A1. Subsequent propagation steps A2, A9, acid−base reactions A10−A12, quenching the OH radical in B2, and the B3 feed-back reaction are considered to be very fast. Thus, a steady-state approach can be used for HO_2^-, O_3^-, OH, and CO_3^- and standard derivation yields the following rate law:

$$\frac{d[O_3]}{dt} = -1.5k_1[O_3][OH^-] \quad (4)$$

Under the conditions applied here, $[OH^-] \gg [O_3]$, the rate law is consistent with experimental observations and predicts first-order decay for ozone,

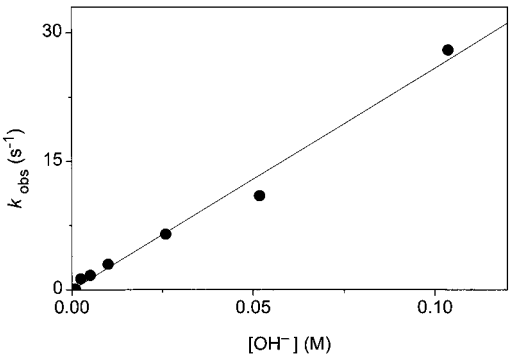

Figure 3. Pseudo-first-order rate constant, k_{obs}, for carbonate ion inhibited decomposition of ozone as a function of $[OH^-]$; $t = 25$ °C, $I = 0.5$ M $NaClO_4$.

$$\frac{d[O_3]}{dt} = -k_{obs}[O_3] \quad (5)$$

where $k_{obs} = 1.5\ k_1[OH^-]$. As expected, the plot of the measured pseudo-first-order rate constant, k_{obs}, as a function of $[OH^-]$ gives a straight line with zero intercept (Figure 3).

From the slope k_1 was calculated to be 173 ± 9 M^{-1} s^{-1}. This value compares very well with $k_1 = 140$ M^{-1} s^{-1} reported for the NFG model (Table 2). The primary importance of this result is that it provides additional information for the initiation step. Values reported earlier for k_1 are in the range of 40−140 M^{-1} s^{-1}.[6,8,10,12,13] To some extent this variation reflects how the feed-back reactions and kinetic coupling between the propagation steps were considered in the evaluation of the experimental data. Perhaps, the kinetic studies at high carbonate ion concentration provide the best estimates so far for k_1 because the kinetics of the system is substantially simplified under these conditions. In our ongoing studies we attempt to find other inhibitors of ozone decomposition which will act similarly toward carbonate ion. Kinetic studies in the presence of efficient radical scavengers are expected to confirm the conclusions reported in this paper.

Summary. The kinetic model reported in Tables 2 and 3 is consistent with the experimental data under a variety of experimental conditions. It is capable of reproducing the concentration vs time profiles not only for ozone but also for several transient species, such as O_3^-, O_2^-, and CO_3^-. According to a recent report, the carbonate ion radical may efficiently compete with the hydroxyl radical in the degradation of pollutants in waters containing carbonate ion.[35] The model presented here can be used as a basis for the evaluation of the kinetic role of these radicals in oxidation reactions of ozone and may contribute to a quantitative interpretation of the chemical principles of advanced oxidation processes.

Acknowledgment. We thank Dr. Gábor Peintler of Szeged, Hungary, for the software used in the calculations. We are also indebted to Prof. Gilbert Gordon (Miami University, Oxford, Ohio) who brought our attention to the problems addressed in this paper. This work was supported by the Hungarian National Research Foundation under grant No. OTKA M 028244 and T 029568 and by a NATO Linkage Grant under grant No. CRG.LG 973337. Financial support from the Alexander von Humboldt Foundation (I. F.) and a fellowship provided by the Deutsche Akademische Austauschdienst (DAAD) for A. Nemes is also appreciated.

References and Notes

(1) Razumovski, S. D.; Zaikov, G. E. *Ozone and its Reactions with Organic Compounds*; Elsevier: New York, 1984; Vol. 15.

(2) White, G. C. *Handbook of Chlorination and Alternative Disinfectants*; Van Nostrand Reinhold: New York, 1992.

(3) Taube, H.; Bray, W. C. *J. Am. Chem. Soc.* **1940**, *62*, 3357.

(4) Bühler, R. E.; Staehelin, J.; Hoigné, J. *J. Phys. Chem.* **1984**, *88*, 2560.

(5) Masten, S. J.; Hoigné, J. *Ozone Sci. Eng.* **1992**, *14*, 197.

(6) Staehelin, J.; Hoigné, J. *Environ. Sci. Technol.* **1982**, *16*, 676.

(7) Staehelin, J.; Bühler, R. E.; Hoigné, J. *J. Phys. Chem.* **1984**, *88*, 5999.

(8) Tomiyasu, H.; Fukutomi, H.; Gordon, G. *Inorg. Chem.* **1985**, *24*, 2962.

(9) Fábián, I. *Prog. Nuclear Energy* **1995**, *29*, 167.

(10) Chelkowska, K.; Grasso, D.; Fábián, I.; Gordon, G. *Ozone Sci. Eng.* **1992**, *14*, 33.

(11) Nemes, A.; Fábián, I.; Gordon, G. *Ozone Sci. Eng.* **2000**, *22*, 287.

(12) Nemes, A.; Fábián, I.; Gordon, G. *Inorg. React. Mech.* **2000**, in press.

(13) Forni, L.; Bahnemann, D.; Hart, E. J. *J. Phys. Chem.* **1982**, *86*, 255.

(14) Sehested, K.; Corfitzen, H.; Holcman, J.; Hart, E. J. *J. Phys. Chem. A* **1998**, *102*, 2667.

(15) Wittmann, G.; Ilisz, I.; Dombi, A. Mechanism of Catalysed Ozone Decomposition in Aqueous Solutions. *Proceedings of the Regional Conference on Ozone, Ultraviolet Light, Advanced Oxidation Processes in Water Treatment*; 1996, Amsterdam, The Netherlands.

(16) Nelson, S. L.; Carter, L. E."A Process Using Ozonated Water Solutions to Remove Photoresist After Metallization. *Proceedings of the International Symposium on Ultra Clean Processing of Silicon Surfaces* (UCPSS), 1998.

(17) Hong, A.; Zappi, M. E.; Kuo, C. H.; Hill, D. *J. Environ. Eng.* **1996**, *122*, 58.

(18) Buxton, G. V.; Greenstock, C. L.; Helman, W. P.; Ross, A. B. *J. Phys. Chem. Ref. Data* **1988**, *17*, 513.

(19) Holcman, J.; Sehested, K.; Bjergbakke, E.; Hart, E. J. *J. Phys. Chem.* **1982**, *86*, 2069.

(20) Tonomura, B.; Nakatani, H.; Ohnishi, M.; Yamaguchi-Ito, J.; Hiromi, K. *Anal. Biochem.* **1978**, *84*, 370.

(21) Czapski, G. *J. Phys. Chem.* **1967**, *71*, 1683.

(22) Czapski, G.; Dorfman, L. M. *J. Phys. Chem.* **1964**, *68*, 1169.

(23) Weeks, J. L.; Rabani, J. *J. Phys. Chem.* **1966**, *70*, 2100.

(24) Peintler, G. *ZITA 4.1: A Comprehensive Program Package for Fitting Parameters of Chemical Reaction Mechanisms*, Szeged, Hungary, 1990.

(25) Hindmarsh, A. C. *GEAR: Ordinary Differential Equation Solver, Rev. 2*; Lawrence Livermore Laboratory, 1972.

(26) Czapski, G.; Samuni, A.; Yellin, R. *Isr. J. Chem.* **1968**, *6*, 969.

(27) Rizzuti, L.; Augugliaro, V.; Marrucci, G. *Chem. Eng. Sci.* **1976**, *31*, 877.

(28) Christensen, H.; Sehested, K.; Corfitzen, H. *J. Phys. Chem.* **1982**, *86*, 1588.

(29) Eigen, M.; DeMaeyer, L. *Z. Electrochem.* **1955**, *59*, 986.

(30) Buxton, G. V.; Wood, N. D.; Dyster, S. *J. Chem. Soc., Faraday Trans 1* **1988**, *84*, 1113.

(31) Ross, A. B.; Neta, P. *Natl. Stand. Ref. Data Ser., Natl. Bur. Stand.* **1979**, *65*, 62.

(32) Behar, D.; Czapski, G.; Duchovny, I. *J. Phys. Chem.* **1970**, *74*, 2206.

(33) Buxton, G. V. *J. Chem. Soc., Faraday Trans.* **1969**, *68*, 2150.

(34) Farhataziz; Ross, A. B. *Natl. Stand. Ref. Data Ser., Natl. Bur. Stand.* **1977**, *59*, 113.

(35) Umschlag, T.; Herrmann, H. *Acta Hydrochim. Hydrobiol.* **1999**, *27*, 214.